sciendo

ANNALS OF WEST UNIVERSITY OF TIMISOARA PHYSICS
Vol. LXIII, 2021

DOI: 10.2478/awutp-2021-0006

Ag CONTINUOUS DOPED SnO_2 SENSOR SELECTIVE TO CO_2 IN PRESENCE OF ETHANOL AT ROOM TEMPERATURE

M'hammed Benali Benadjemia [1, 2,*], Mourad Lounis [2], Mohamed Miloudi [3], Nabil Beloufa [4]

[1] *Electronics Engineering Department, Mohamed Boudiaf University, Oran, Algeria*
[2] *GIDD Laboratory, Electrotechnical & Automatic Engineering Department, University of Relizane, Algeria*
[3] *APELEC Laboratory, Electrotechnical & Automatic Engineering Department, University of Relizane, Algeria*
[4] *LaMiN Laboratory, National Polytechnic School, Oran, Algeria*
**Corresponding author: mhammedbenali.benadjemia@univ-relizane.dz*

Article Info	Abstract
Received: 02.06.2021 *Accepted: 01.09.2021* **Keywords:** Gas sensor; Room temperature operation; Catalyst.	This paper contains experimental research to minimize the basic limits of the SnO_2 semiconductor oxide gas sensor. The operating temperature is high. In addition, their selectivity diminishes with gasses having the same chemical behavior. An experimental methodology is presented to overcome the difficulties of these metal oxides. The efficiency of the gas sensors made of Ag continuously doped at room temperature is excellent. At the end of the testing processes and security measures supplied, laboratory tests and experiments will be conducted to guarantee the acceptability of the planned study.

1. Introduction

One of the principal factors acting on the gas sensor's performance is the operating temperature. It is generally rather high (T > 300 °C). An operation at high temperatures induces the development of its physical-chemical properties instead of increasing the energy consumption needed for heating a sensitive element. This inevitably induces a drift of the long-term electrical responses. This high temperature can also pose problems of thermal degradation of the gas molecules to be detected. It also limits explosive gas detection. This can be a source of an explosion due to the sensor itself. In addition, high temperatures may degrade circuit performance if the sensor comes on the same silicon die [1]. For all these reasons one of the

essential factors for the development of effective chemical sensors for useable energy and stability appears to be the capacity to detect gas at an environmental temperature [2].

Several studies have demonstrated that SnO_2 can detect different oxidizing gasses or reduce them at ambient temperature [3,4]. Besides the temperature disadvantage, the decrease in selectivity for gasses with the same chemical behavior is taken into account. The crossing of sensitivity enters the ethanol, CO_2, and CH_4 presented by P. Breuil *et al.* [5]. This weakness poses significant problems in producing a gas sensor for a household. This effort aims to have a selective sensor at a very low temperature of around 20 °C along this axis. Many studies [6,7] provide one of the most recognized and used ways for the addition of catalytic materials for improving the selection of gas sensors [8].

In this work, we exploited two ways of deposition of Ag due to its low cost and good performance. The first deposition of Ag is the dispersed way, which is much quoted in [6,9,10]. The second procedure is the continuous deposit of Ag which is quoted little by the literature. CO_2 is considered one of the main greenhouse gases. For instance, fossil fuels, solid wastes, in addition to some specific chemical reactions [11]. Gone are numerous research [12-14] preparing doped SnO_2 films and catalytic coatings that address that problem, since the highly stable CO_2 gas showed a poor response when reacted with pure SnO_2 metal oxide film [12]. Driving drunken drive power, fermentation monitoring, and other chemical processes are required for the production of a highly sensitive sensor. Ethanol is associated with high volatility and flame retardation. It might be humanly and lively toxic as well. The development of thin film-based ethanol sensors offers the advantages of greater sensitivity [4,12].

The study suggests a comprehensive method for prediction. There are also numerous tasks using an analytical expression. The thin layer of 0.5 μm of SnO_2 has been applied to a dopant or a catalyst of silver (Ag). It is done in an atmosphere at room temperatures of 20, 40, and 60 °C by the electrolysis method. Additionally, the relative humidity of 30 %, for two target gases oxidant and reduced 7 ppm for CO_2 and 20 ppm for ethanol 95 %.

2. Experimental study

The following process was used for the preparation of SnO_2 films: 2 g chloride dihydrate ($SnCl_2$–$2H_2O$) was dissolved in 15 mL of C_2H_5OH. At 75 °C – 80 °C for one hour the solution was agitated using magnetic stirring equipment. The solution was then combined with the glycerine ($C_3H_8O_3$) to provide the sol-gel for dip-coating as a dispersal stabilizer. This approach favored the application for the dip-coating technique of films from the solution (sol). Substrate glass slides of [76×26×1] mm are cleaned for five minutes and lastly, we rinse with

ethanols by immersing them in the ultrasound bath. Both films are dipped in the soil and removed slowly at a set pace of 80 mm/min from the bathroom. All the films have been dried for 30 minutes at a low temperature of 100 °C. They are then heat-treated for 60 minutes at 500 °C. The crystalline structure of SnO_2 films has been investigated by the use of an X-ray diffraction system (Shimadzu XRD diffraction) with CuKα1 radiation λ = 1.54 Å, at 30 kV/30 mA. Fizeau interferometer used a He-Ne laser (0.5 μm) to measured film thickness.

For solutions prepared for silver deposition on the SnO_2 layer, the solution is made up of 36 g/L silver cyanide, 60 g/L cyanide potassium (sodium), 45 g/L carbonates, potassium (sodium), and 0.75 mg/L carbon disulfide. By analysis: 28.7 g/L silver, and 43 g/L free potassium cyanide. We used an agitation cathode preferred (cathode efficiency is 100 %) and anode silver with the following conditions: temperature is 24–32 °C, the current density is 0.5–15 A/dm^2, ratio anode to cathode area is 1:1, and voltage < 6 V. The transparent conductive oxides (SnO_2) represents cathode.

The first prototype, injected ethanol 95 % gas (Fig. 1) is made of a glass chamber of dimension [85×85×47] mm with a small opening to make circulate the gas, the chamber is used to contain gas injected by the means of a gas pipeline. The quantity of ethanol injected is the same for all the experiments 20 ppm. The transparent conductive oxides (TCO), substrate glass slides on which deposited us a layer of SnO_2 a thickness of 0.5 μm inside the chamber (Fig. 2). On the thin layer, we have deposited silver Ag in two separate, scattered, and continuous ways using the electrolysis process. A beaker to contain the ethanol, a thermometer to measure the boiling point of ethanol (78.3 °C), a heating resistance supplied with a voltage supply to heat SnO_2 and a thermometer in direct contact with the thin layer controls the temperature (the relative humidity is 30 %).

The second prototype, injected CO_2 gas (Fig. 1) is made of the same glass chambers and transparent conductive oxides (TCO) for the prototype. For this experience, we injected CO_2 gas into the chamber. We utilized the same method as the SnO_2 heating prototype, measure the conductance, the electrodes of measurement, and control temperature. The quantity of CO_2 injected into the chamber is the same for all the experiments at 7 ppm. 10 mg/m^3 for gas of CO_2 gives 9 ppm (1 mg/m^3 = 0.873 ppm). After each experiment we rinse the chamber with the air, the time of coverage is approximately 30 s. The amounts identified in ppm will be assessed by the difference in ethanol levels in each experiment before and after each experiment (after evaporation). The duration of each exposure to the ethanol vapor is 15 s. The quantity injected is 20 ppm into the chamber is the same one for all the experiments. Typical ethanol

injection of 0.4 mL is the gas concentration of approximately 10 ppm. The coverage time is around 30 s after each experiment when we clean the chamber by air.

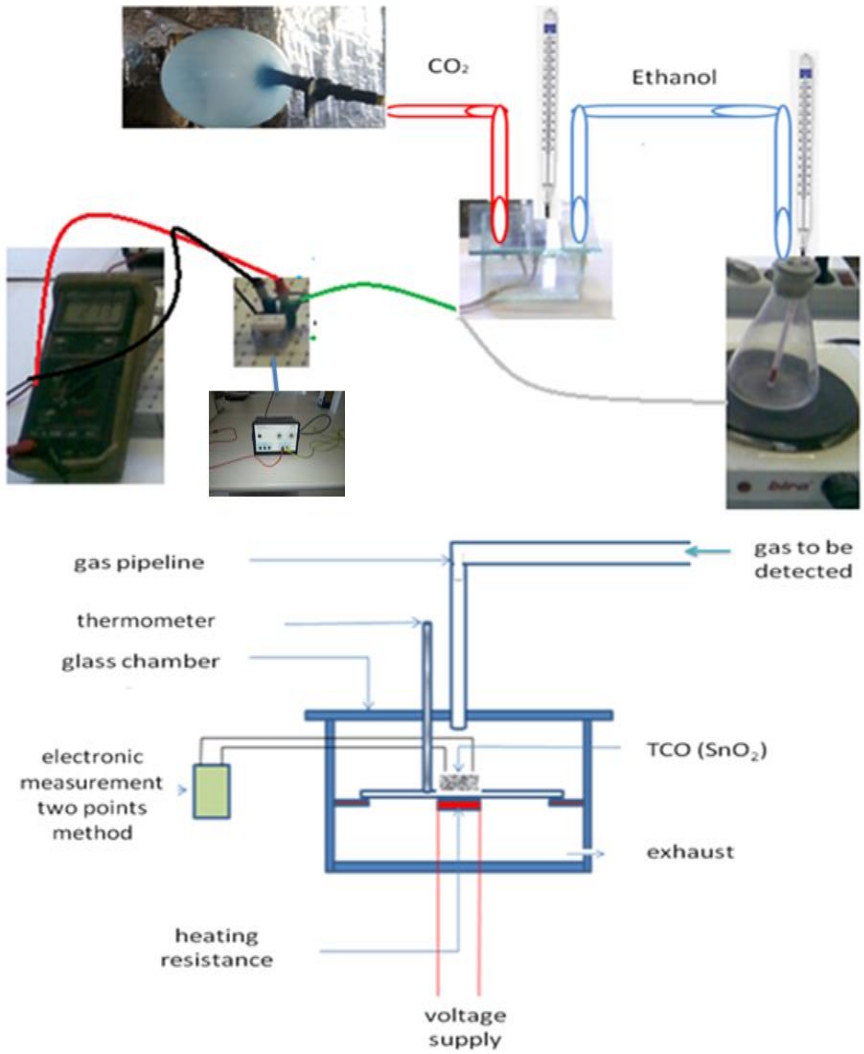

Figure 1. Experimental and Detailed diagram of the various parts of the experimental devices to detect gas.

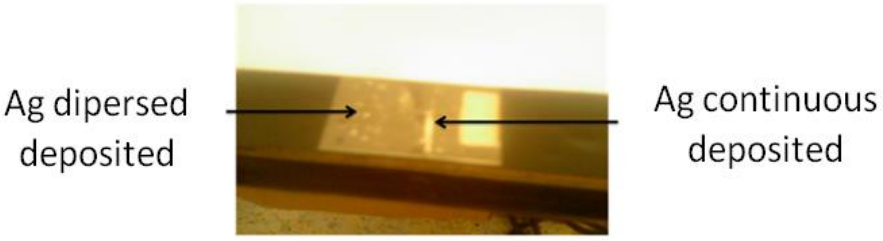

Figure 2. TCO with Ag continuous and dispersed doped SnO_2.

The electrodes of the combs of measurement between alume digitalization are depicted in Fig. 3 to take the least variation of the leading process into consideration.

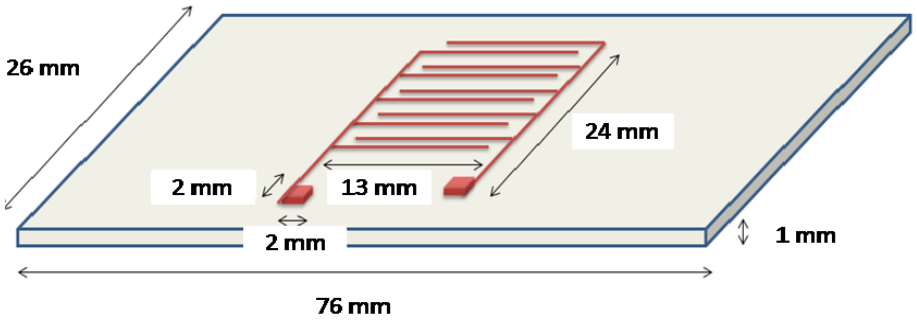

Figure 3. Electrodes of aluminum combs inter digitizes for measurement.

The percolation procedures for every semi-conductor sample or structure (lines of transport of current). In principle, the connections between transport routes and semi-conductors let the current go in both directions and have the least contact resistance feasible. The resistance of a contact R is defined by equation (1). Whereas, R_C is the specific resistance of contact ($\Omega.cm^2$) and A is the surface of the contact. We can decrease this resistance by increasing the surface of the contact.

$$R = \frac{R_C}{A} \tag{1}$$

It is therefore interesting to digitize on the surface of sensitive layers to improve electrical measurements (reduction in resistances of contact). This applies especially if the layers are highly resistant or if you are unable to do so. In addition, the catalytic effect might prove to be fascinating. The electrode can nonetheless be formed using metal particles. The electrodes can usually be made of gold or platinum but sometimes of tungsten, silver, or aluminium. In this last case, they are specially reserved for use at low temperatures.

We have utilized the two-point methodology shown in Fig. 4 to measure the conductance. Furthermore, we made measurements of the resistance R_s of our thin layer once under air and once again under gas. This takes place to calculate the sensitivity S of our sensor during these experiments. Then, we calculated the conductance for both gases. To find the resistance R_s we measured the voltage V_L at the boundaries of the resistance charges R_L. The choice of the value of the resistance R_L is ten times less than the resistance R_s value to take the least variation of the resistance R_s (Fig. 4) (supply voltage V = 3 V).

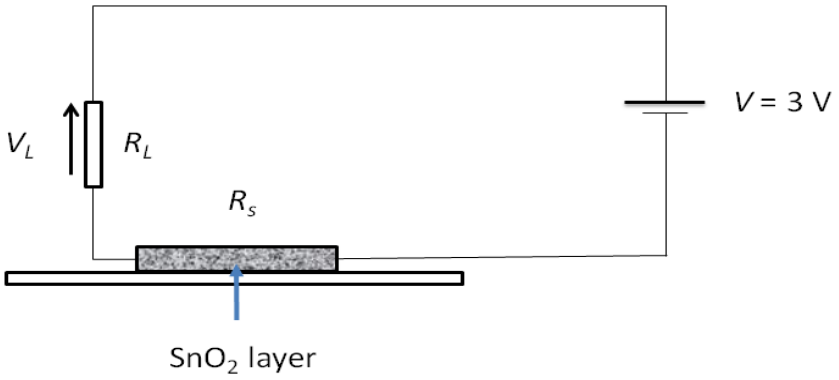

Figure 4. Method of the two points to measure the conductance.

$$V_L = \frac{R_L}{R_L + R_S} V \tag{2}$$

$$R_S = R_L\left(\frac{V}{V_L} - 1\right) \tag{3}$$

The relative response of the sensor (also called sensitivity) was defined as:

$$S = \frac{G_0 - G}{G_0} \tag{4}$$

Where G is the conductance under gas and G_0 is the conductance under air. If $G_0 > G$ we apply the definition of equation (4) and if $G > G_0$, the order of G and G_0 must be reversed to have S positive.

3. Experimental Results and discussions

For our sensor, according to Fig. 5, we notice that there is a sensitivity for small quantities 7 and 20 ppm for CO_2, and ethanol respectively at low temperatures. Ethanol in general reacts by adsorbing oxygen, but the temperature for oxygen reactions is sufficient.

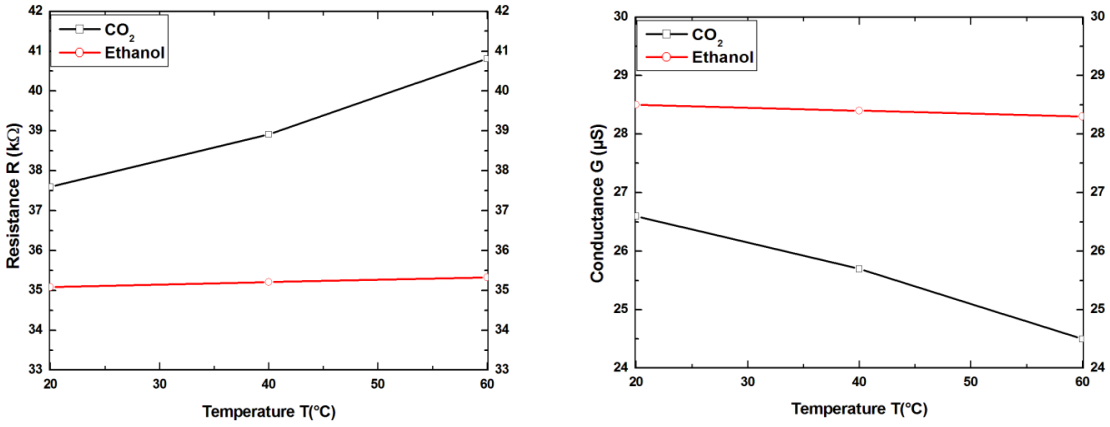

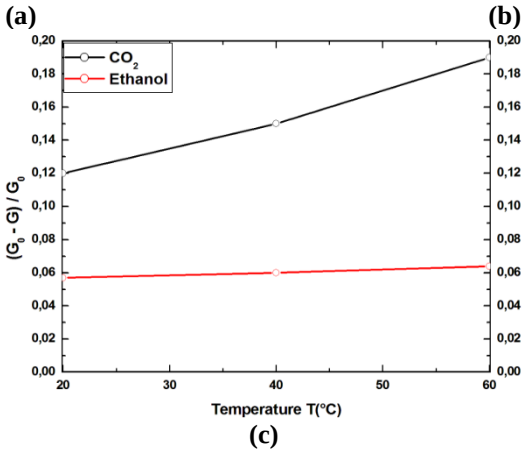

Figure 5. (a) The resistance; (b) The conductance; and (c) The relative sensor responsiveness in the presence of low-temperature ethanol and CO_2.

The ions of orbed oxygen (O_2) on the SnO_2 sensing surface can form various species, respective to the operation temperature as shown in the following equations [15]:

For T < 100 °C: $$O_2(gas) \rightarrow O_2(ads) \quad (5)$$

For T > 100 °C: $$O_2(ads) + e^- \rightarrow O_2^-(ads) \quad (6)$$

$$O_2^-(ads) + e^- \rightarrow 2O^-(ads) \quad (7)$$

In our case, to clarify the sensor detecting method at low temperatures 20, 40, and 60 °C, at room temperatures below 70 °C, the sensors' performance changes considerably from that of their counterparts at high temperatures. When the sensors were exposed to C_2H_5OH steam, their conductivity was reduced. The unique response of the reducing gasses at room temperature is that oxygen molecules are binding at lower (room) temperature oxygen vacancies exclusively to localized electrons. When an ethanol molecule adsorbs on the surface of the nanowire it interacts with oxygen vacancies directly with electrons situated, resulting in donor site impairment. This is based on the following equation:

$$C_2H_5OH(gas) + e^- \leftrightarrow C_2H_5OH^- \quad (8)$$

The current in the nanostructure will drop [16]. The electrons left behind in states where the energies sit near the conduction band and operate as n-type contributors are located when vacancies are produced. Thus, the development of vacancies typically considerably boosts oxide conductivity. Furthermore, the oxide surface of atoms or molecules prefers to bond to vacancies of oxygen. When the adsorbed molecules accept the chemical bonds to the surface (for example ethanol), they use the electrons located on the vacancy site. This reduces the conductivity of the n-type oxide by the adsorption of an electron acceptor. The molecules

interacted with oxygen from the surface, removed it, created low donor conditions, and increased conductivity [17].

It also cites that the electrons are liberated after exposure to chemicals such as ammonia through interactions between reduced gas and negative oxygen adsorbents. It then helps to reduce resistance [18]. However, for the gas sensing under 70 °C, the opposite behavior was found. The sensor film's resistance increases when ammonia gas is exposed. The positive (abnormal) and negative (ordinary) reactions at low and high operating temperatures are synthesized for this variation. This is understood. The probable sensing mechanism for ethanol can be explained by the following equations [19]:

$$C_2H_5OH_{(gas)} \leftrightarrow C_2H_5OH_{(ads)} \quad (9)$$

$$C_2H_5OH_{(ads)} \leftrightarrow C_2H_5O^- + H^+ \quad (10)$$

$$C_2H_5O^- + h^+ \leftrightarrow C_2H_5O_{(ads)} \quad (11)$$

$$H^+ + e^- \leftrightarrow H_{(ads)} \quad (12)$$

Where $C_2H_5O^-$ is the ethoxy group ion, H^+ is hydrogen ion, h^+ is the positive hole, and e^- is electron [19].

For CO_2, we notice that there is a response at low temperatures. The sensor forms little oxygen species due to low thermal energy when operating at room temperature. Owing to the great energy of the adsorption, thermally stable and difficult to remove from the soil is this relatively limited number of oxygen species. Relative moisture (RH) is also one of the major disruptive factors of the gas sensor operating at room temperature.

As the RH level increases, the number of oxygen species will fall [20]. The dissociated hydroxy and hydrogen ions of the water molecule reaction on the surface of metal oxide at low temperatures to gaseous CO_2 have been described by [21] Ostrich *et al*. This is to form carbonate ions CO_3^{2-} as given in equations (13–17), with the intermediate products, formate ions, and bicarbonate ions [21].

$$H_2O \leftrightarrow OH^- + H^+ \quad (13)$$

$$CO_{2(gas)} + OH^-_{(adsorbed)} \leftrightarrow HCO^-_{3(surface)} \quad (14)$$

$$CO_{2(gas)} + H^+_{(adsorbed)} + 2e^-_{(surface)} \rightarrow HCO^-_{2(surface)} \quad (15)$$

$$HCO^-_{2(surface)} \rightarrow CO \uparrow + OH^-_{(\text{surface})} \quad (16)$$

$$HCO_{3(surface)}^{-} + OH^{-}{}_{(adsorbed)} \leftrightarrow CO_{3(bulk)}^{2-} + H_2O_{(gas/surface)} \quad (17)$$

Fig. 6 shows that the dissipated silver addition enhances the sensitivity. This is done by way of ethanol at a temperature of 20 °C, with a factor times more than 1.43 for the deposit. A metal catalyst can enhance the kinetics of surface reactions.

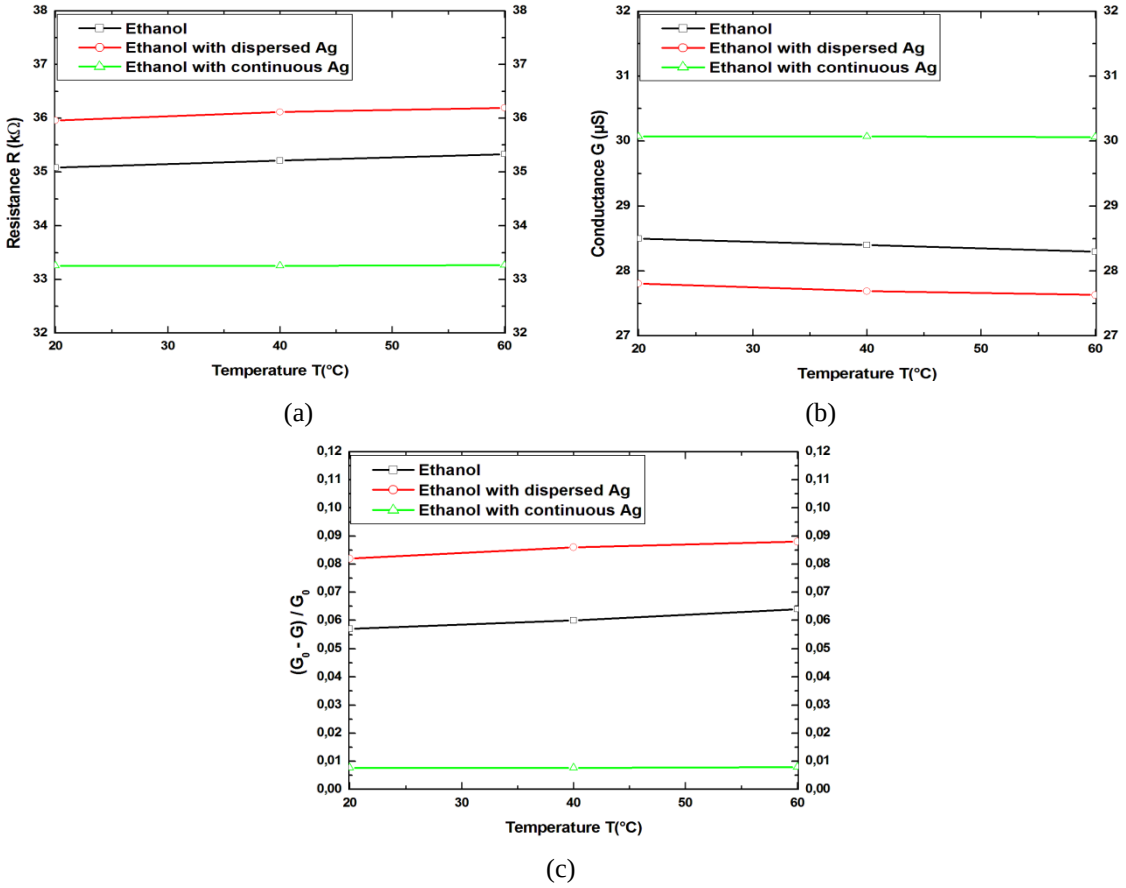

Figure 6. (a) The resistance; (b) The conductance; and (c) The sensor's relative responsiveness with and without the injection of ethanol at low temperatures.

Various methods are offered nowadays to characterize the synergy between metal and SnO_2. The mechanism which we want to use in our situation is S. Morrison's electrical effect mechanism [22] that is valid for the silver [12]. This notion is based on an electric metal exchange and the semiconductor started this mechanism. It reports on the adsorption through electronic transmission of oxygen on the surface of the metal. We notice in the first chemisorption of oxygen. In this case, oxygen takes electrons with metal. It is according to the equation (18).

$$O_2(gas) + 2\,e_M + 2\,s_M \rightarrow 2O^- - s_M \quad (18)$$

e_M and s_M represent respectively an electron and a site of adsorption of metal. Oxygen remains adsorbed on metal. An electrical disruption to the SnO_2/metal Interface was caused by this negatively charged adsorbed phase. The disturbance that would result in an exchange of electrons between two materials according to the equation (19):

$$e_{OX} \rightarrow e_M \tag{19}$$

There still, this loss of electrons leads to the alteration in this substance of the space charge zone. In the event of RH_2 gas reduction, on the surface of the catalyst, one attends his oxidation. This is according to equation (20).

$$RH_2(gas) + 2O^- - s_M \rightarrow RO(gas) + H_2O(gas) + 2e_M + 2s_M \tag{20}$$

And consequently, an electron is returned to oxide:

$$e_M \rightarrow e_{OX} \tag{21}$$

$$C_2H_5OH(gas) + 2O^- - s_M \rightarrow CH_3CHO(ads) + H_2O(gas) + 2e_M + 2s_M \tag{22}$$

One of the main parameters controlling the gas sensitivity of materials may recognizably be found in the sensor operating temperature. The answer is low, it may be observed. At low temperatures, the relatively low reactivity is primarily due to the little amount of oxygen adsorbed on the surface of the material. As the temperature increases, the kinetics of chemical oxygen reactions on the surface of the sensing material grow quicker. In addition, sufficient energy is gained from the target gas molecules. This means overcoming the barrier to activating energy and reacting with oxygen adsorbent atoms.

Furthermore, here is discussed the thin film room temperature sensor for the Ag-SnO_2. As SnO_2 is a key element for determining sensitivity Ag atoms replace Sn atoms in Ag-doped SnO_2. This reduces the energy gap. In addition, thin-film has greater adsorption energy than pure SnO_2 film. There can be a lesser energy gap, as there is a comparably lower silver energy gap in tin oxide. It contributes greatly to the sensitivity of the sensor manufactured at room temperature. Ag doping in SnO_2 doping also reduces grain size and increases the efficient area of the surface. It also results in reduced sensitivity to temperatures [23].

Besides, the areas under the surface of the metal surface may mix if the Ag is appropriately scattered by a thin layer of SnO_2. It contributes substantially to the mechanism

of electrical interaction. This process is therefore significantly below 100 °C in electrical contact. This can also contribute to the sensitivity of ambient temperature [23]. Noble metal Ag doping affects the shift to lower temperatures of the optimum operating temperature. Yet, it is due to a decrease in the bandgap. The calculated Energy Gap (Eg) of Ag-doped SnO_2 was much less than that of pure SnO_2, because of introducing Ag impurities. Consequently, The electrical valence band (VB) transition to the conductive band (CB) has been achieved in Ag-doped SnO_2 more easily than in pure SnO_2 [24].

The sensitivity to ethanol for the deposit is continuously reduced significantly. Hence, the partial link between Ag and/or Ag particles may be ascribed. The sensitivity was significantly lower; with factor times lower of 0.13 at 20 and 60 °C respectively. Thus, the whole relation between metallic Ag and/or Ag layers is revealed. The sensor resistance is not dictated by the gas detecting capabilities of SnO_2 when the Ag Islands are partly or linked. However, the insensitive conducting Ag layer is identified instead. The development of conduction channels via the ag-layers is hence responsible for low or no gas response in the Ag-SnO_2 sensors [25].

The Ag surfactant will cover the raw material at a higher Ag level. The surface-active sites are also resistant to gas. Hence, the gas response decreases for H_2S reduced gas [26]. The H_2S-reduced doped sensor gas response decreased at 3.0 mol percent Ag, probably by a drop in the active sites associated with the agglomeration of Ag grains [27].

For CO_2, according to Fig. 7, the addition of the silver improved the sensitivity with a factor times higher of 1.66 and 2.33 and for dispersed and continuous way respectively for 20 °C. The additive catalyzes the sensing materials' surface carbonation. It also supports the device's performance as a metal injection source. The addition of metal to a carbon dioxide sensor can increase its responsiveness based on past studies.

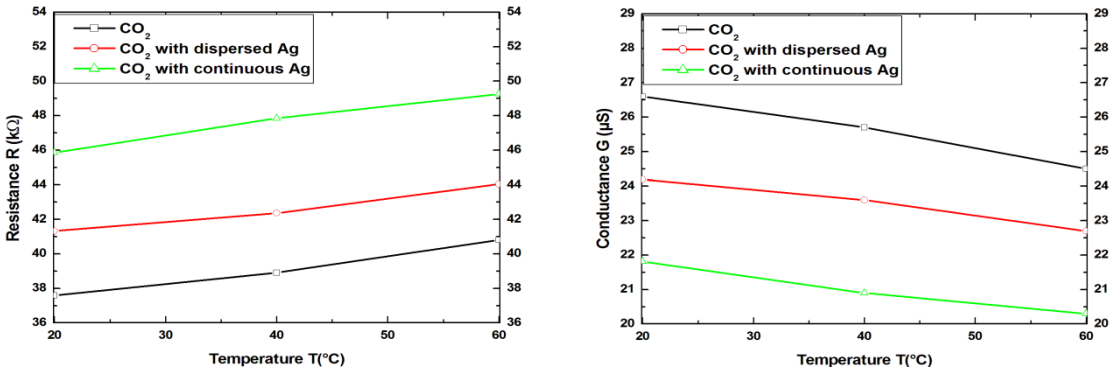

(a) (b)

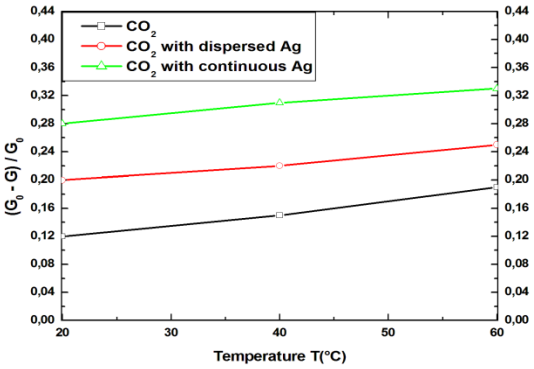

(c)

Figure 7. (a) The resistance; (b) The conductance; and (c) The relative response of the sensor to CO_2 with and without metal addition according to low temperatures.

These improvements can be explained by the existence of the dispersed doping agent, regardless of what is more substantial than the ethanol component. But for the way continues we can say that there were more reactions between CO_2 and oxide what it can be with the significant presence of the doping agent. Hence, it has to accelerate the reactions of CO_2 with oxide. Also, the Ag metal boosts sensor layer chemical activity and boosts CO_2 adsorption. The small size of the CO_2 molecule can be also the cause that allows the molecules CO_2 to infiltrate. Which, takes place between the islands formed by the silver continuous. This reverses it for the ethanol, which has a gross molecule.

We can attribute this good response also to the formation of small Ag_2O/Ag clusters cited by [28] for PdO/Pd for CO. They are bound to the surface of the tin dioxide. It is likely to lead to and potentially alter CO_2 oxidation on the surface of nanocomposites. Hence, it is supported by the alteration of the response–temperature dependence.

The difference between the two gaseous curves exhibits practically a likeness in Fig. 8 for the doping agent distributed to that in Fig. 6. Thus, this is explained by the same improvement of two gases sensitivity in the presence of the dispersed doping agent, with a factor of 1.43 and 1.66 respectively for CO_2 and ethanol at 20 °C.

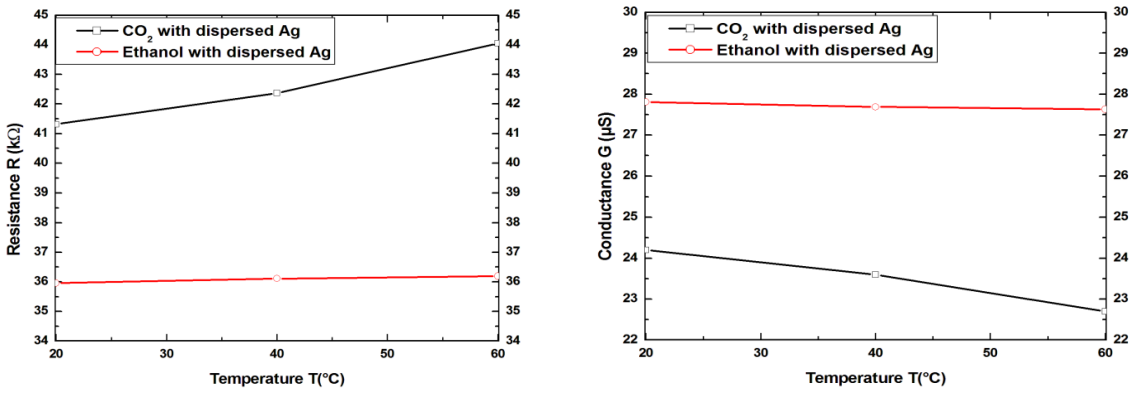

(a) (b)

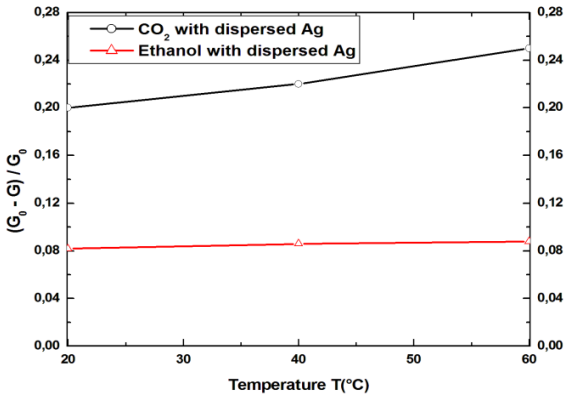

(c)

Figure 8. (a) The resistance; (b) The conductance; and (c) The relative response of the sensor to ethanol and CO_2 with metal addition dispersed according to low temperatures.

The consequence of the ongoing doping agent is shown in Fig. 9. We see that there is a considerable discrepancy between the two gas curves. Hence, it is with a factor times lower of 36.36 and 41.25 between two gases (CO_2/ethanol) respectively for 20 °C and 60 °C. The presence of catalysts continuously improved the sensitivity of CO_2 to the detriment of ethanol.

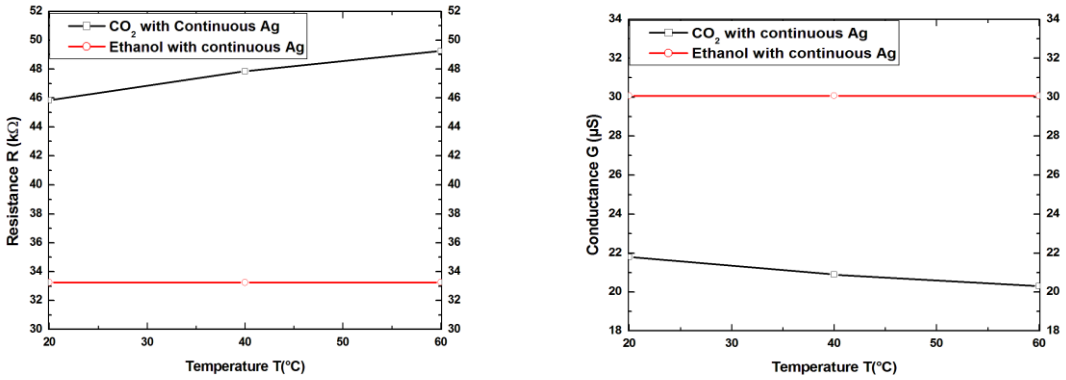

(a) (b)

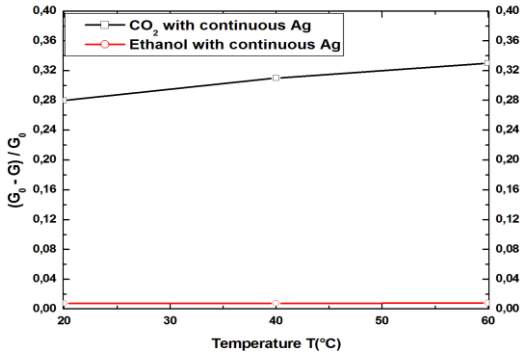

(c)

Figure 9. (a) The resistance; (b) The conductance; and (c) The relative response of the sensor to ethanol and CO_2 with metal addition continuous according to low temperatures.

In Fig. 10, we find clearly that adding the doping agent and the method the doping agent is deposited may be a selecting factor in the presence of ethanol to detection of CO_2.

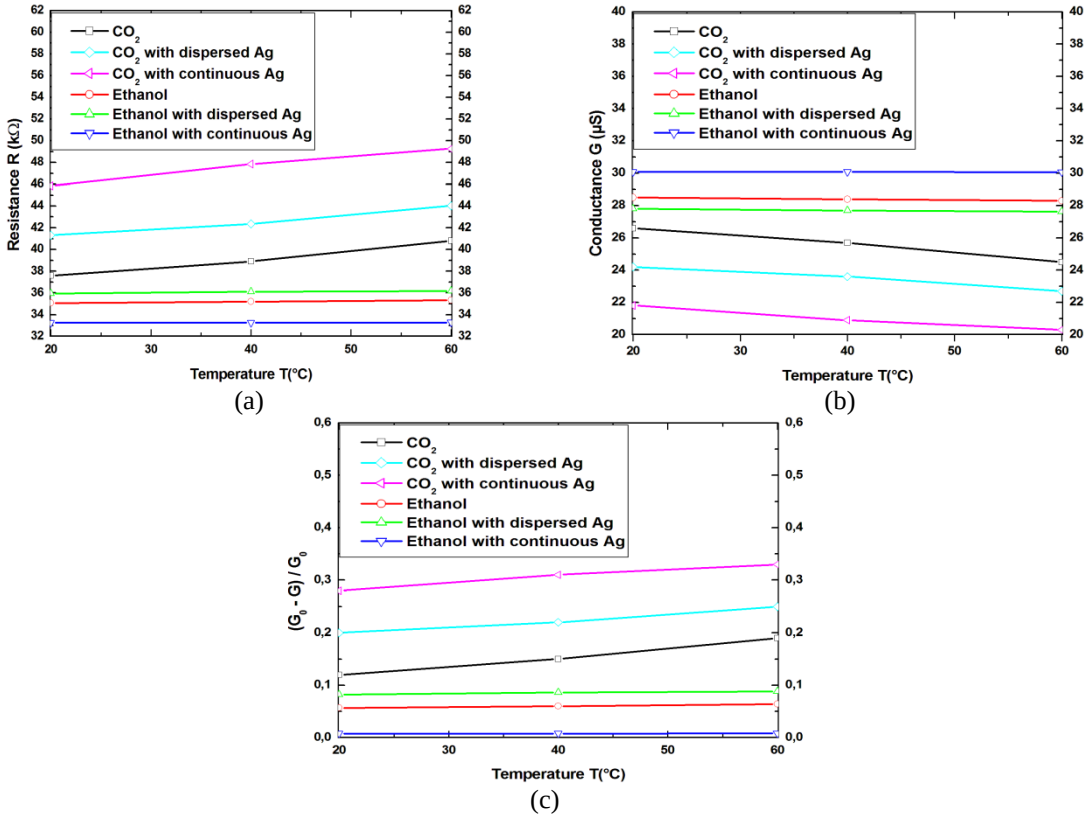

Figure 10. (a) The resistance; (b) The conductance; and (c) The relative response of the sensor to ethanol and CO_2 without and with metal addition dispersed and continuous according to low temperature.

4. Conclusion

In this study, we've been interested in the SnO_2 gas sensor. Besides, we posed the problems of metallic oxides. SnO_2 for us who are not selectivity and the operating temperature, which is rather high. To solve the problems of these metallic oxides, we made a series of experiments, while working with low temperatures 20, 40, and 60 °C. Then, we have remade the same experiments. However, this time in the presence of a doping agent. That is the silver by depositing it on oxide by the electrolysis method. It takes place once in a dispersed way, and a second continuously.

According to the found results, we can have a sensitivity of our metallic oxide to low temperatures. The addition of the doping agent silver in a way dispersed increases the sensitivity for two gases but its presence continuously improved the sensitivity of CO_2 significantly what is not for ethanol. Then, we can say that our continued deposited doping has led our sensor to selectivity by detecting CO_2. This is a gas standard source that represents the greenhouse effect at the expense of ethanol.

Acknowledgments

The authors would like to thank the staff of the Electronic Microscope and Materials Science Laboratory at Oran University for their help in carrying out this work.

References

[1] R. Ghosh, JW. Gardner and PK. Guha, IEEE Transactions on Electron Devices, 66.8 (2019) 3254.

[2] A. Gaddari, M. Amjoud, F. Berger, J.B. Sanchez, el all, EDP Sciences, (2013) 04010.

[3] N. Bhardwaj, S. Mohapatra, Ceramics International, 42.15 (2016) 17237.

[4] A. Mirzaei, S.G. Leonardi, G. Neri Ceramics International. 42.14 (2016) 15119.

[5] P. Breuil, N. Perdreau, C. Pijolat, Analusis, 28.7 (2000) 633.

[6] G.E. Patil, D.D. Kajale, V.B. Gaikwad, N.K. Pawar, Sensors & Transducers Journal, 137.2 (2012) 47.

[7] L. Zhu, W. Zeng, Sensors and Actuators A, 267 (2017) 242.

[8] A. Cabot, J. Arbiol, J.R. Morante, U. Weimar, N. Barsan, W. Gopel, Sensors and Actuators B: Chemical, 70 (2000) 87.

[9] P. Tyagi, A. Sharma, M. Tomar, V. Gupta, Chem Sensors, 4 (2014) 18.

[10] A. Sharma, M. Tomar, V. Gupta, J. Nanosci Lett, 2 (2014) 27.

[11] M.A. Basyooni, S.E. Zaki, S. Ertugrul, M. Yilmaz, Y.R. Eker, Ceramics International, 46.7 (2020) 9839.

[12] Prabakaran Shankar, John Bosco Balaguru Rayapan ,A review. Sci. Lett.4.4 (2015) 126.

[13] Shravanti Joshi, Samuel J Ippolito, Selvakannan R. Periasamy, Ylias M. Sabri, and Manorama V. Sunkara, ACS Appl. Mater. Interfaces 32 (2018).

[14] Qing Li, Jiaju Fu, Wenlei Zhu, Zhengzheng Chen, Bo Shen, Liheng Wu, Zheng Xi, Tanyuan Wang, Gang Lu, Jun-Jie Zhu, and Shouheng Sun, Am. , Chem Soc.12 (2017) 4290.

[15] A. Beniwal, Journal of Materials Science: Materials in Electronics, 30.3 (2019) 3144.

[16] C. H. Xu & H. F. Lui & C. Surya, J Electroceram, 28.1 (2012) 27.

[17] Y. Zhang, A. Kolmakov, S. Chretien, H. Metiu and M. Moskovits, , Nano letters , 4(3) (2004) 403-407

[18] Y.S Kim, S.C Ha, K Kim, H Yang, S.Y Choi, and Y. TKim, applied physics letters 86 (2005) 21.

[19] A Beniwal, P.K Sahu, S. Sharma, Journal of Sol-Gel Science and Technology, 88 (2018) 2.

[20] L Zhu, W Zeng, Sensors and Actuators, 17(2017)242.

[21] B Ostrick, M Fleischer, H Meixner, Sensors and Actuators B: Chemical 68 (2000) 1-3

[22] S. Morrison, Selectivity in semiconductor gas sensors, Sensors and Actuators 12(1987) 4.

[23] A Beniwal, S Lalwani, and Sunny, AIP Conference Proceedings 1 (2009) 020039.

[24] P. S. Kolhe, P M. Koinkar, N Maiti, K M. Sonawane, Physica B: Condensed Matter 524(2017) 90–96.

[25] R.J Wu, D.J Lin, M.RYu, M.H Chen, H.F. Lai, Sensors and Actuators B 178(2013) 185.

[26] D. N. Chavan, G. E. Patil, D. D. Kajale, V. B. Gaikwad, P. K. Khanna, and G. H. Jain, Journal of Sensors, (2011) 1.

[27] P.S. Kolhe, P.M. Koinkar, N.Maiti, K.M. Sonawane, Physica B 524 (2017) 90.

[28] A V.Marikutsa, M. N.Rumyantseva, L.V.Yashina, A. M. Gaskov, Journal of Solid State Chemistry.183(2010) 10.